Facilities for X-ray Optics Calibration

Bianca Salmaso, Alberto Moretti, and Jessica Gaskin

Contents

B. Salmaso (✉)
INAF Astronomical Observatory Brera, Merate, Lecco, Italy
e-mail: bianca.salmaso@inaf.it

A. Moretti
INAF Astronomical Observatory Brera, Milano, Italy
e-mail: alberto.moretti@inaf.it

J. Gaskin
NASA Marshall Space Flight Center, Huntsville, AL, USA
e-mail: jessica.gaskin@nasa.gov

C. Bambi, A. Santangelo (eds.), *Handbook of X-ray and Gamma-ray Astrophysics*,
https://doi.org/10.1007/978-981-16-4544-0_14-1

Abstract

Before launching an X-ray observatory, the performance of a telescope mirror or mirror assembly in the X-ray energy band of interest must be determined. This calibration requires a specialized facility that can approximate an astronomical point source and accommodate the mirrors and other telescope components, including an appropriate detector system. The X-ray source and telescope are typically housed in a vacuum chamber to permit easy propagation of the X-rays. X-ray test facilities around the world are being used to calibrate flagship and smaller X-ray observatories for multiple space agencies. These facilities are also regularly used to support the development of new types of optics for future missions. In this chapter, we describe currently available facilities and list some of the key missions that used them for calibration. Future facility developments needed to support the next-generation X-ray missions are also discussed.

Keywords

X-ray optics · X-ray telescope · X-ray calibration · X-ray sources · Beamline

Introduction

X-ray mirrors and mirror assemblies need to be tested during their development and for the final calibration. Accurate calibration of the effective area and determination of the point spread function (PSF) in the focal plane drives the test facility requirements.

X Versus UV Light

X-ray light needs to be used, as UV light produces diffraction effects that can enlarge the PSF. It is worth mentioning that UV light was used in the past, as in the case of XMM Newton, as a complementary test to the X-ray calibration (Stockman et al., 1999; Tock et al., 1988). A UV facility is also under construction for the integration of the ATHENA telescope, using the accurate determination of the barycenter, to measure the PSF of mirror sub-assemblies to be integrated (Valsecchi et al., 2021b).

Source Distance

Ideally, one would like to calibrate the optics on the ground under the same conditions that they would operate in space. This requires approximating a point source, typically achieved by placing the X-ray source as far as possible from the optics to be tested. The finite distance of the source, S, causes the true focal length, f_{true}, to be slightly longer than the nominal focal length, f_{nom}, as given by the Lens-Maker equation:

$$\frac{1}{f_{\mathrm{true}}} = \frac{1}{f_{\mathrm{nom}}} - \frac{1}{S}, \tag{1}$$

The measured-to-nominal focal length ratio decreases with increasing source distance and decreases with decreasing f_{nom} (Fig. 1).

Moreover, a divergent beam, produced by a source at finite distance, will not necessarily fully illuminate the first sector of the X-ray telescopes. This problem gets worse with increasing focal length (Basso et al., 2007) and results in a loss of the measured effective area. The measured fraction of effective area increases with longer S and decreases with increasing nominal focal length (see Fig. 2, which shows the case of an X-ray mirror approximated by a double cone).

Vacuum

As the transmission of X-rays in air is low, especially for soft X-rays, the facility must operate in vacuum. As large optics need large facilities, the evacuation time plays an important role.

A complement of facilities exists globally that were used to calibrate past and currently flying X-ray missions and that are currently available for future testing and calibration (Table 1). In the following sections, we describe those facilities, dividing them in three regions: Europe in section "Europe," Unites States in section "United

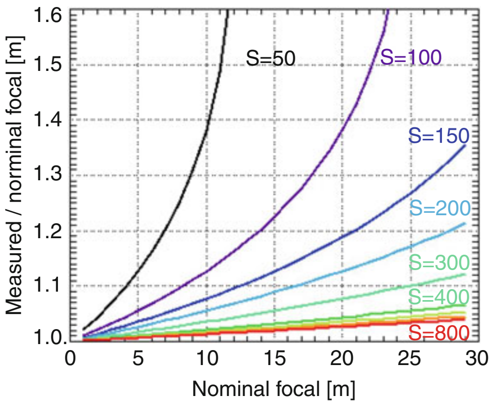

Fig. 1 Image distance to nominal focal length ratio versus nominal focal length for different source to detector distances S

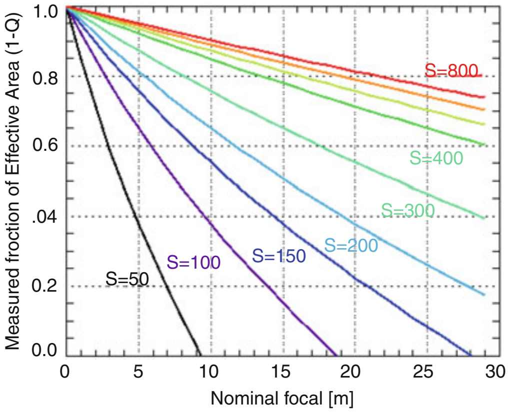

Fig. 2 Fraction of the measured effective area for mirrors with double cone geometry, for different source to detector distances *S*

States," and Asia in section "Asia." Section "Synchrotron Radiation Facilities" provides an overview of the synchrotron radiation facilities, as they are also regularly used for X-ray optics calibration. General observations regarding existing facilities are provided in section "Remarks Concerning Existing X-ray Facilities." The last section is dedicated to two new capabilities that are under development: BEaTriX (Beam Expander Testing X-ray facility) and VERT-X (Vertical X-ray facility). These facilities are nontraditional and introduce new ideas for calibrating X-ray optics.

Europe

The PANTER X-Ray Test Facility at MPE (Germany)

PANTER was originally built at the end of the 1970s for developing high-quality X-ray mirrors. In 1982, the 120 m long, 1 m diameter vacuum tube, was set up for the testing of the ROSAT optics, together with a vacuum chamber (3.5 m diameter and 6 m long) ideal for testing its f = 2.4 m telescope mirror with shells with diameter up to 0.84 m. Since then, the facility was used for many projects, including EXOSAT, BeppoSAX, JET-X, XMM-Newton, Swift, Suzaku, eROSITA, International X-ray Observatory (IXO), and the Advanced Telescope for High ENergy Astrophysics (ATHENA). To adapt to the different missions, several upgrades were performed during these years. In the 1990s, a new chamber was built (3.5 m diameter and 12 m long) to calibrate the f = 7.5 m and 0.7 m diameter optics of the XMM-Newton mission. In 2012 (Burwitz et al., 2013), an extension was setup at PANTER to enable the calibration of the f = 20 m optics (IXO mission). After that, PANTER was upgraded to measure the f =12 m optics of ATHENA (Burwitz et al., 2017).

This facility is considered a reference calibration facility for X-ray optics in Europe. It was built by MPE (Garching, Germany), and it is located in Neuried, close to Munich. Figure 3 shows the aerial view with the long vacuum tube, connecting the X-ray source at the right end to the test vacuum chamber on the left side.

Table 1 X-ray telescopes and the existing X-ray calibration facility used for their calibration. This is a representative sampling of missions and is not inclusive

Year of launch	Mission	Led by	X-ray test facility
1978	Einstein Observatory	NASA	XRCF
1983	EXOSAT LE	ESA	Laboratory for space research, The Netherlands
1990	ROSAT XRT-WFC	DLR	PANTER
1993	ASCA	JAXA	ISAS
1996	BeppoSAX MECS-LECS	ASI	PANTER
1999	Chandra	NASA	XRCF
1999	XMM-Newton EPIC	ESA	PANTER
2004	Swift XRT	NASA	PANTER
2005	Suzaku XRT	JAXA	ISAS
2012	NuSTAR	NASA	[a]RaMCaF
2015	AstroSat SXT	ISRO	Indus-1 synchrotron
2016	Hitomi SXT	JAXA	GSFC 100-m + ISAS + SPring-8
2017	HXMT LE	CAS	IHEP 100-m
2019	SRG eROSITA	IKI/DLR	PANTER
2019	SRG ART-XC	IKI/DLR	MSFC 100-m, IKI 60-m
2021	IXPE	NASA	MSFC 100-m
2023	XRISM	JAXA	GSFC 100-m
2023	SVOM MXT	CNSA/CNES	PANTER
2023	SVOM WXT	CNSA/CNES	LLBTF
2023	Einstein Probe FXT	CAS	PANTER + IHEP 100-m
2027	eXTP SFA-SFA	CAS	IHEP 100-m
Early 2030s	ATHENA	ESA	XRCF + PANTER + XPBF 2.0 at BESSY II
			BEaTriX + VERT-X

[a]The Neil Rainwater Memorial Calibration Facility (RaMCaF) is no longer in operation

Fig. 3 An aerial view of the PANTER X-ray test facility. (Credit: MPE/PANTER)

The PANTER X-ray source is a multi-target open electron beam impact source which, combined with 2 filter wheels, allows for fast switching between anodes. A list of the standard X-ray calibration lines is given in Table 2.

Table 2 PANTER calibration line. (Credit: MPE/PANTER)

Line	Energy (keV)	Line	Energy (keV)
B K_α	0.18	Ag L_β	3.26
C K_α	0.28	Ti K_α	4.52
O K_α	0.53	Ti K_β	4.94
Cu L_α	0.93	Cr K_α	5.42
Al K_α	1.49	Fe K_α	6.41
Si K_α	1.74	Cu K_α	8.06
Ag L_α	3.00	Ge K_α	9.90

Due to the long, but finite distance of the source, the beam is not parallel. Two Fresnel zone plates (Menz et al., 2015) were designed and fabricated to collimate the divergent X-ray beam, for the Al-K_α emission line at E = 1.49 keV. For the 4-inch zone plate, the measured angular resolution was ±0.2 arcsec for the first order diffraction; for the 6-inch zone plate, ±0.5 arcsec angular resolution was obtained.

Two detectors are available at PANTER: the Third Roentgen Photon Imaging Counter (TRoPIC, 19.2 mm size, 75 μm pixel), a smaller eROSITA prototype CCD, and the Princeton Instruments X-ray Imager (PIXI) (about 27 mm size, 20 μm pixel). Also an AMPTEK SDD is used as a monitor counter; it is located about 35 m from the X-ray source to monitor the source stability and check the beam homogeneity.

The vacuum in this facility reaches 10^{-7} mbar, necessary to make measurements at very low energies ($E < 1$ keV). Due to the large instrument vacuum chamber, a long evacuation and venting time is needed.

In order to maintain the cleanliness of the optics when the vacuum is broken, the instrument chamber is connected to a clean room.

In addition to testing and calibrating X-ray optics, gratings, filters, detectors, and complete X-ray telescopes have been tested (see Fig. 4) at PANTER. For the approved Chinese-European missions Einstein Probe and SVOM, the Flight Model (FM) optics and the FM Telescope have been tested, respectively. The Einstein Probe Follow-up X-ray Telescope FM and combination of ATHENA Mirror Modules in a petal and a critical angle transmission (CAT) grating tested together for the Arcus mission are shown in Fig. 5, mounted in the vacuum chamber.

The XACT Facility at Palermo (Italy)

The X-ray Astronomy Calibration and Testing (XACT) facility of Istituto Nazionale di AstroFisica (INAF) – Osservatorio Astronomico di Palermo (AOP) is located in Palermo (Italy) (Barbera et al., 2006). It was built in 1990 to support the development and calibration of the UV/Ion shields of the High Resolution Camera (HRC) on board the Chandra X-ray Observatory. Since then, the facility has been used for the testing and calibration of filters and detectors of several projects such as XMM-Newton, JET-X, ROSAT, and Solar-B. The facility has also been used for

Fig. 4 End-to-end tests in PANTER. (Left) The eROSITA FM telescope entering the PANTER vacuum chamber. (Right) The SVOM-MXT-FM positioned in the PANTER vacuum chamber. (Credit: MPE/PANTER)

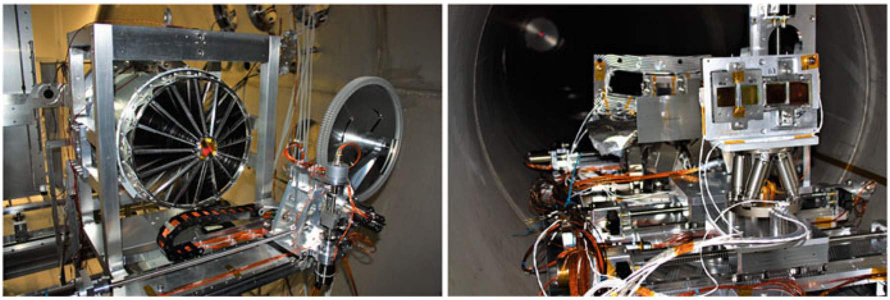

Fig. 5 Testing optics and gratings in PANTER. (Left) The Einstein Probe QM Mirror Module. (Right) An ATHENA SPO petal combined with a CAT grating petal for the Arcus GWAT test on the extended optical bench in the 1 m diameter beamline tube. (Credit: MPE/PANTER)

developing grazing incidence X-ray optics, such as lobster eye optics, thin plastic foil optics, and thin glass foil optics with active control (Figs. 6 and 7) (Schnopper et al., 2003; Tichy et al., 2011; Spiga et al., 2016).

The vacuum pumping system is entirely based on magnetic levitation turbo-molecular pumps and on oil-free rotary pre-vacuum and back-up pumps. A minimum pressure of 5×10^{-8} mbar can be achieved, while normal operation is in the 10^{-7} mbar scale.

The X-ray source is located at the rightmost end of the beamline shown in Fig. 6. The monochromator is placed in the chamber that is connected to the X-ray source. A vacuum tube with increasing diameter connects the monochromator chamber to the test chamber, to allow a full area illumination of 800 mm diameter. The telescope test chamber is 3.5 m long and 1 m diameter. To the extreme left of the beamline, the detector test chamber is present, with length of 1 m and diameter of 1 m.

The facility can be equipped with different sources, monochromators, and detectors to allow measurements from the UV to soft X-rays. Table 3 summarizes the available components. All the details can be found in Barbera et al. (2006).

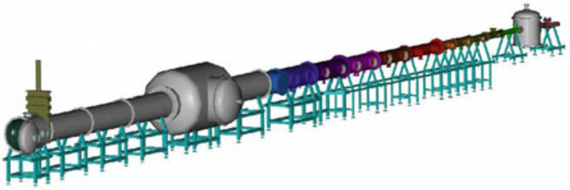

Fig. 6 Schematic drawing of the XACT facility. To the extreme right, the X-ray source is present. From right to left, the monochromator chamber, the telescope test chamber, and the detector test chamber. (Credit: INAF-OAPA)

Fig. 7 (Left) An active X-ray glass mirror mounted in XACT. (Right) An X-ray plastic mirror mounted in XACT. (Credit: INAF)

Table 3 Sources, monochromators, detectors available at the XACT facility (Barbera et al., 2006)

Wavelength [Å]	Sources	Monochromators	Detectors
1–100	Electron Impact X-ray Source	Transmission Grating Double Diffraction Grazing Incidence Reflection Grating	Gas Flow Prop. Gas Scintill. Prop. Counter Micro-Channel Plate Si PiN Solid State Detector
50–350	Gas Discharge Penning Source	Grazing Incidence Reflection Grating	Micro-channel Plate Windowless Photodiode
300–1200	Gas Discharge Hollow Cathode	Grazing Incidence Reflection Grating	Micro-channel Plate Windowless Photodiode
1100–3000	Gas Discharge Hollow Cathode Mercury Lamp	Grazing Incidence Reflection Grating	FUV Photomultiplier Tube Windowless Photodiode Silicon Photodiode

Several vacuum-compatible positioning systems are present to operate the double diffraction monochromator, to align the X-ray optics, and to move slits, filters, pinholes, and the detectors inside the detector chamber.

The XACT facility allows the test and calibration of grazing incidence optics with moderate angular resolution (FWHM $>$ 10 arcsec), outer diameter $<$ 700 mm, and focal length < 10 m. Due to the relatively short distance between the source and the optics under test, the fraction of the telescope lost for double reflection is considerable, making it well-suited for telescope development rather than for telescope calibration.

The Leicester Long Beamline Test Facility (UK)

The Long Beamline Test Facility (LLBTF) at the University of Leicester was designed and built to test X-ray optics and detectors and has been used to test and calibrate instruments for many missions including ROSAT, XMM-Newton, Swift, Bepi-Colombo, and SVOM. It has recently been used in the calibration of the SVOM MXT optic and for the thermal calibration of a WXT loster-eye telescope module, part of the Einstein Probe mission payload. The facility consists of a 28 m long X-ray tube, departing from a 2 × 1.5 m experimental chamber located in an ISO-6 (class 1,000) clean room. Inside the chamber, the optic under test can be moved by a Gimbal system for accurate positioning and rotating. Both fully integrated instruments, like the Bepi-Colombo Mercury Imaging X-ray Spectrometer (MIXS) and smaller individual optics, such as Micro Pore Optics (MPOs), can be located in this chamber. In the case of testing individual MPOs, the Gimbal mechanism is capable of mounting up to 6 individual optics on a rotating carousel allowing them to be tested in a single pump-down cycle.

The two imaging detectors, an MCP and CCD, are positioned side by side and are moved independently in three linear dimensions by in-vacuum linear motors. The vacuum is provided by a turbo-molecular cryopump and is capable of achieving pressures $\sim 5\ 10^{-7}$ mbar. The source can be isolated from the beamline so that either part can be vented independently.

Two X-ray sources are available. The soft X-ray source covers the energy range from C-K (0.28 keV) to Ti-K (4.51 keV). The hard X-ray source is capable of producing X-rays of up to ∼100 keV. It can be configured to stimulate X-ray florescence of external targets providing a wide range of possible X-ray energies but at the cost of significantly reduced count rates and hence longer integration times. The facility is capable of doing controlled thermal tests and can actively control the temperature of the optics under test and the mounting structures. Figure 8 shows the source and the detector ends of the facility.

The IKI 60 m X-ray Facility (Russia)

The X-ray facility of the Space Research Institute of the Russian Academy of Sciences (IKI) was built in 2008. Since then, it has been modernized and re-equipped several times. It was recently used in 2016–2017 for the test campaign on the ART-XC mirror system and detector unit on the Spectrum-Rontgen-Gamma (SRG) mission (Pavlinsky et al., 2018) (Fig. 9).

Fig. 8 (Left) The tube and the X-ray source end. (Right) The vacuum chamber from outside. (Credit: UL)

Fig. 9 (Left) The SGR ART-XC optics installed onto the hexapod inside of the vacuum chamber. (Right) The ART-XC detector placed onto an at the focus of the mirror system. (Credit: IKI)

The IKI X-ray test facility consists of a 60 m long vacuum tube and a test chamber of 4 m length and 1 m diameter. The vacuum tube has two sections of different diameters. The first 15-meter section starts from the test chamber and has an inner diameter of 600 mm. The second 45-meter section has an inner diameter of 309 mm.

The pneumatic vacuum gate is installed on the vacuum tube a few meters away from the vacuum chamber and allows one to achieve the operational vacuum level in the test chamber within one working day (Fig. 10).

Within the vacuum chamber, optics (or optical assemblies) and a detector can be positioned on two vacuum-compatible hexapods, allowing movement in 6 degrees of freedom.

The X-ray flux is monitored using Amptek XR-100SDD and XR-100T-CdTe detectors with a 5×5 mm^2 sensitive areas.

The X-ray beam is produced using interchangeable X-ray tubes with different targets. A 37.5 mm manual vacuum gate valve is installed to enable the replacement of the X-ray tube with minimal downtime. Operations can resume typically within an hour.

Fig. 10 (Left) The vacuum chamber positioned in a ISO-8 clean room. (Right) A micro-focus Oxford Instruments X-ray tube with a manual vacuum gate valve and a pumping unit. (Credit: IKI)

United States

X-ray and Cryogenic Facility at MSFC (Huntsville, AL)

The MSFC X-ray and Cryogenic Facility (XRCF) has provided flagship-level calibration for over four decades. Previously called the X-ray Calibration Facility, it was built in the mid-1970s to calibrate the High Energy Astrophysical Observatory (HEAO). The facility was essentially rebuilt in 1990 to calibrate the Chandra X-ray Observatory and then modified again in 1999 to support a large cryogenic shroud, capable of reaching temperatures down to < 20 K, for direct incidence cryo-mirror development. From 2005–2013, the XRCF supported calibration of the James Webb Space Telescope (JWST) (Kegley et al., 2006). Preparations to support the calibration of the ATHENA telescope are ongoing. In addition to supporting these large flagship missions, the XRCF supports numerous smaller missions and technology developments across astrophysics and heliophysics.

The facility (shown in Fig. 11) consists of a building that houses multiple X-ray sources, a 518 m long by 1.5 m diameter guide tube, and a large, $\sim$7 m diameter by $\sim$23 m long, instrument chamber that opens into a 557 m^2, ISO6 (Class 1k) cleanroom. The chamber's seismically isolated test volume is temperature controlled from $-129\,°C$ to $+93\,°C$ (55 zones). The total source to detector distance is 538 m. The current configuration accommodates full-illumination testing of 1.46 m diameter optics with focal lengths up to 15 m (O'Dell et al., 2004). The achievable vacuum is on the order of 10^{-7} mbar, allowing for the relatively unimpeded propagation of X-rays from the source to detector. Additionally, the facility is equipped with a helium refrigeration system and several helium-cooled enclosures to enable instrument and optic evaluation at temperatures from $< -254\,°C$ to $+49\,°C$.

Test article alignment is accomplished via a telescope and laser coincident with the X-ray axis. Test article receiving and processing is aided by a 20-Ton lift platform located in a 232 m^2 enclosed unloading room. A 186 m^2 ISO7

Fig. 11 (Top-Left) XRCF at MSFC. The source is located in the building on the upper-left of the image and the instrument chamber and clean room is the large building in the lower right. The beamline is 518 m long and roughly 1.5 m in diameter. (Lower-Left) Portion of the James Webb Space Telescope undergoing testing in the XRCF. (Right) The Chandra X-ray Telescope being prepped for calibration inside the facility. (Credit: NASA MSFC)

(Class 10k) cleanroom serves as the facility's "airlock." The ISO6 (Class 1k) cleanroom is served by a 20-Ton overhead crane. Other notable capabilities include a 1.2 m × 2.4 m cryogenic-optical test chamber, a 1.2 m × 2.4 m preconditioning chamber, a 1.2 m × 1.2 m contamination evaluation chamber, and a 372 m^2 fabrication shop and assembly building. X-ray beamline and optical capabilities are summarized in Table 4.

The 100-m X-ray Facility at MSFC (Huntsville, AL)

The NASA Marshall Space Flight Center (MSFC) 100-m X-ray Beamline, also known as the Stray Light Test Facility (SLTF), was built in 1963 and has supported numerous technology developments and missions over the years. One of the earliest efforts was supporting the development and testing of a stray light suppression system for the Large Space Telescope (LST) (Wyman et al., 1975). LST eventually evolved into the Hubble Space Telescope (HST). Since this time, the facility has been used to primarily test X-ray optics, optical assemblies, instrumentation, and complete observatories (Thomas et al., 2021). Most recently, the Imaging X-ray Polarimetry Explorer (IXPE) was calibrated there (Baumgartner et al., 2021).

The facility, located on Redstone Arsenal in Huntsville, AL, is just over 100-m long and features a large, 3-m diameter and 8-m long, instrument chamber that is

Table 4 Summary of XRCF capabilities for X-ray and Optical testing

Type	Capability	Description
In-chamber system	Seismically insulated test rail system	Two 3.0 m × 3.7 m optical benches
	Precision alignment tables	6 degree-of-freedom table (1,360 kg capacity) Size: 1.2 m × 1.8 m Cryogenic/vacuum operation Five axis mount (998 kg capacity) Size: 1.2 m × 2.4 m Vacuum operation
X-ray test capabilities	Beamline	518 m long x 1.5 m dia Pressure $< 1.3 \times 10^{-7}$ mbar Beam dia. = 1.46 m; divergence = 1.39 mrad half-angle Knife-edge apertures along length to ensure a pure, unreflected beam from source to test optic or instrument
	X-ray source	Seismically isolated Electron Impact Point Source Rotating-anode sources Filter chamber and wheel Custom/other sources readily accommodated
	X-ray beam monitors/ mappers	Flow proportional counters and silicon drift detectors on 2D stages 50 m from source and at the chamber entrance
	Focal plane detectors	18 m focal length (longer is possible) Focal plane detector system Flow proportional counters, silicon drift detectors CCDs and commercial planar detectors Custom/other detectors readily accommodated
Direct incidence optical test capabilities	Optical test window	273 mm clear aperture N-BK7 window Tilt capable: ±6° pitch/yaw
	Metrology positioning & alignment and	Polytech PI Hexapod Aerotech X,Y,Z translation stages
	Metrology instruments	4D PhaseCam Leica Absolute Distance Meter FLIR thermal imaging camera and associated window Displacement measuring interferometry
	Optical test stability	Seismically insulated ±1 μrad line of sight
	Mirror test capability	Mirror diameters up to 5.3 m (4.2 m to 15 K) Radii of curvature up to 22 m

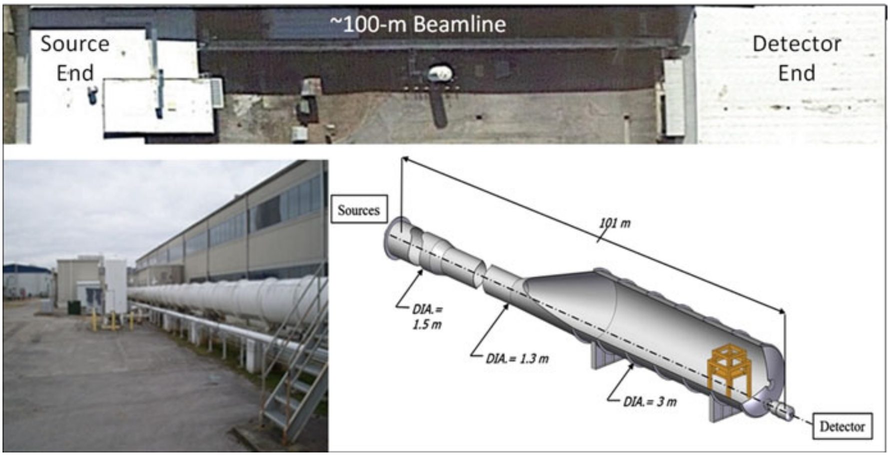

Fig. 12 (Top) Ariel view of the MSFC 100 m beamline. (Lower-Left) Looking down the beamline toward the source end of the facility. (Lower-Right) Schematic of the facility. The relatively large beamline tube diameter and instrument chamber on the detector end of the facility permits testing of large test assemblies. (Credit: NASA MSFC)

ideal for housing fairly large optics, optical assemblies, and detectors with reasonable focal length capability. The beamline tube diameter is 1.3 m at its narrowest point, permitting full illumination of sizable test assemblies. The beamline can support a vacuum as high as 10^{-7} mbar (10^{-5} mbar vacuum can be achieved within 4 hours, from atmosphere). The facility is integrated into a building that houses the MSFC Optics Group and includes multiple metrology labs, polishing machines, and machining capability (Fig. 12).

An auxiliary bell housing (external vacuum chamber) includes internal linear, tip, and tilt stages that can be used to accommodate longer focal lengths and for quick turnaround testing. The bell housing is ∼0.6 m in diameter × ∼1.4 m long and can be installed within a couple of hours (Fig. 13). Additional tubing can also be installed to meet longer focal lengths.

A large area (113 m^2) ISO7 (Class 10K) cleanroom houses the detector end of the facility (Fig. 14). This cleanroom has a 3 Ton overhead crane, gantry crane, high-precision laser range tracker to verify test article positions in the chamber, and continuous temperature monitoring. This room is adjacent to a ISO8 (Class 100K) staging and work area (Fig. 13). The facility also includes a loading dock for easy transport of large test articles.

The source-end of the facility is equipped with a laser alignment system that allows for rough optical alignment of test articles (optics, gratings, etc.) to the detector. This system uses a retractable mirror that reflects the laser down the z-axis of the facility and allows for an X-ray source to be installed without interference (Fig. 15).

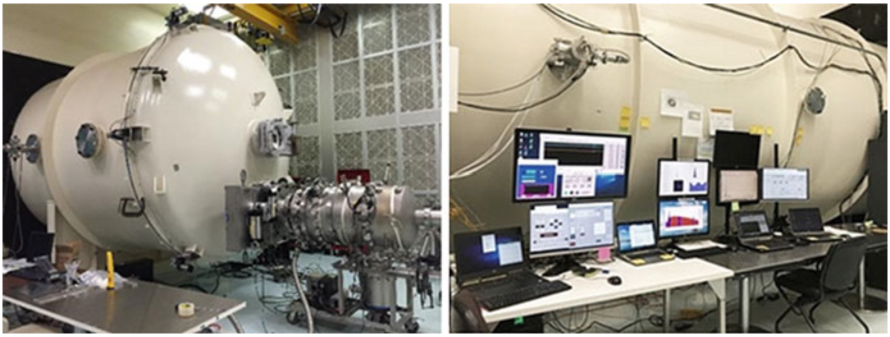

Fig. 13 (Left) Bell housing attached to the end of the MSFC 100 m beamline instrument chamber. The bell housing provides quick turnaround test capability and permits the accommodation of longer focal lengths. (Right) ISO8 (Class 100K) cleanroom and user command and control area. (Credit: NASA MSFC)

Fig. 14 (Left) Instrument chamber dome is removed for test-article integration into the chamber. The chamber is adjacent to an ISO7 (Class 10K) cleanroom. (Right) IXPE mirror module being installed inside the instrument chamber of the MSFC 100 m beamline facility. (Credit: NASA MSFC)

Multiple X-ray sources, detectors, and motion stages provide the capability to support a wide range of test and calibration activities. X-ray active sources include aluminum to tungsten anodes of varying voltages, currents, window thicknesses, and source sizes. A MSFC-built polarized source, used to calibrate the Imaging X-ray Polarimetry Explorer (IXPE), is also available as is a windowless Manson source that includes an array of filters (down to Carbon K_α). Detectors include out-of-vacuum and vacuum-compatible charge-coupled devices (CCDs), silicon drift detectors (SDDs), and CdTe planar detectors. Stages include, but are not limited to, a precision hexapod with high load (80 kg) capacity and linear stages that provide X-Y travel of 0.9 m $\times$ 0.76 m with a resolution of 0.1 μm.

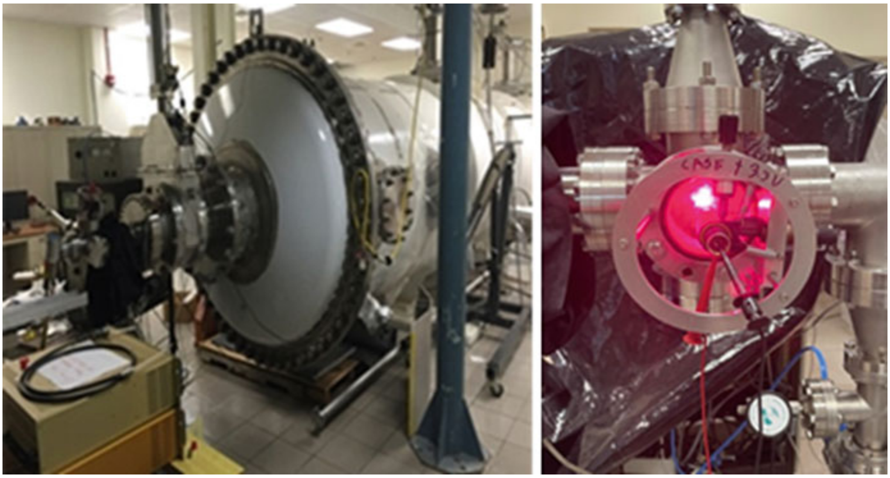

Fig. 15 (Left) Source end of the MSFC 100-m beamline facility. (Right) Laser-alignment system in operation. (Credit: NASA MSFC)

Fig. 16 Image of the GSFC 100-m X-ray beamline showing the X-ray source and instrument buildings. (Credit: NASA GSFC)

The 100-m X-ray Beamline at NASA GSFC (Greenbelt, MD)

The NASA Goddard Space Flight Center (GSFC) 100-m X-ray beamline, built in 2010 and updated in 2019, is located near the Goddard Geophysical and Astronomical Observatory in Greenbelt, Maryland. The beamline, shown in Fig. 16,

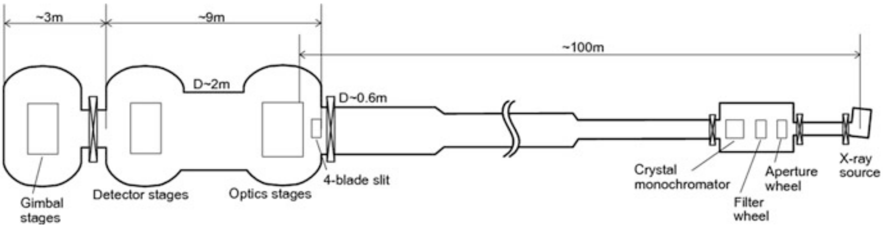

Fig. 17 2D sketch of the GSFC 100-m X-ray beamline. (Credit: NASA GSFC)

supported initial calibration of the Astro-H mirrors (also known as Hitomi) (Iizuka et al., 2018) and test and calibration of the X-ray Imaging and Spectroscopy Mission (XRISM) X-ray Mirror Assembly (XMA) (Tashiro et al., 2020). This capability supported calibration of the Neutron star Interior Explorer Composition Explorer (NICER) flight X-ray concentrator (Okajima et al., 2016) and actively supports research and development of advanced optics and other X-ray instrumentation (e.g., X-ray gratings and detectors).

The beamline is capable of achieving a vacuum of $\sim 10^{-6}$ mbar and can generate a divergent X-ray beam that is 60 cm in diameter as well as a pencil beam that is collimated by a 4-blade slit that is $< 20 \times 20$ mm. The instrument chamber is 2 m in diameter at its largest point, which accommodates the X-ray testing and calibration of mirrors and mirror assemblies that are larger than 60 cm in diameter (Fig. 17). The primary X-ray source is a Rigaku ultraX 18 kW rotating anode X-ray generator (5–60 kV, 10–300 mA). Available anode targets include C, Al, Ti, Fe, Cu, Pt, Mo, Ag, and W. The source filament sizes are 0.1×1 mm, 0.3×3 mm, and 0.5×10 mm. Monochrometers include channel cut crystals suitable for energies < 25 keV and metal filters.

A 5-axis vacuum-compatible stage includes three rotational stages, and a vertical and horizontal linear stage supports mirror actuation during testing. The XRISM mirror assembly is shown mounted on this stage in Fig. 18.

Mirror testing is supported by a 4-axis custom stage assembly that includes a vertical and horizontal linear stages and a rotation stage. Available detectors include Teledyne Princeton Instrument CCD cameras (PI-MTE3 2048B), Amptek SDD, CdTe, and proportional counters.

The 47-m X-ray Beamline at PSU (University Park, PA)

The High Energy Astrophysical Detector and Instrument group at Pennsylvania State University maintains a 47-meter long X-ray calibration facility, including oil-free pumps, mercury-free pressure gauges, multi-anode X-ray sources, and detector control electronics (https://sites.psu.edu/headilab/). This beamline has been used to calibrate and test rocket payloads, including those with the first X-ray CCD flights

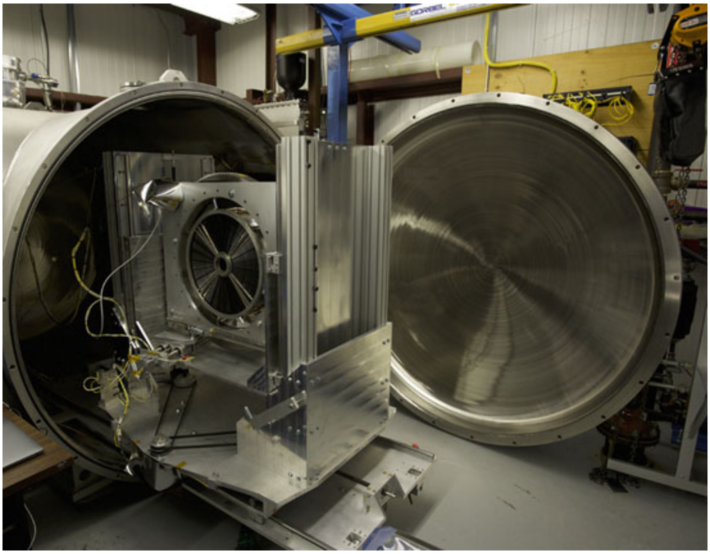

Fig. 18 XRISM mirror mounted on the optics stage being installed into the GSFC 100-m beamline. (Credit: NASA GSFC)

Fig. 19 Instrument end of PSU 47-m long X-ray calibration facility. (Left) Main cryopump mounted to the side of the beamline (black tube, 86-cm diameter). (Right) X-ray test camera mounted onto the vacuum door. Mirrors or entire instruments can be inserted into the 98-cm diameter experiment section. (Credit: PSU)

that observed SN1987A (Burrows et al., 1989) and more recent rocket flights with X-ray hybrid CMOS detector cameras and modern experimental X-ray optics. The chamber is also used for CubeSat calibration and testing, X-ray optics development, X-ray grating developments, and testing and advancement X-ray detectors for the next generation of X-ray orbiting observatories. The instrument end of the X-ray beamline is approximately 1 m in diameter (∼98 cm inner diameter), with a large vacuum door that swings out for easy access (Fig. 19). Externally, this door has a flange and gate valve that provides adaptable experiment and instrument mounting schemes. Large instruments and optics, and even entire rocket or CubeSat payloads, can be inserted completely into the chamber. Alternatively, smaller instruments within their own independent vacuum enclosures, such as cameras and compact CubeSat payloads, can be mounted on standard external chamber flanges with a gate valve in between. Custom and standard feed-throughs are available for electronics and for cooling tubes containing liquid nitrogen. Instruments that are inserted into the 1 m diameter tube can be mounted on a combination of 2 gimbal stages and/or 2 linear stages for precise positioning and control. Along the length of the beamline, there are multiple access ports, including large 22.86 cm (9 inch) ports, as well many small ports and feed-throughs.

The entire 47-m long chamber can hold low pressure vacuum for extended periods of time, enabling long duration experiments and calibration runs, with pressures of $< 3 \times 10^{-6}$ mbar being held for weeks to months at a time. The system uses a CVI TM500 cryogenic pump and 2 CVI TM150 cryopumps to achieve a working pressure within < 4 hours. A nitrogen purge system is also mounted to the beamline.

The source end of the beamline tapers down to a 15.24 cm (6 inch) ConFlat flange with a pneumatic gate valve, on which multiple X-ray sources can be mounted, including a water-cooled multi-anode Henke tube, a Manson tube with interchangeable anodes (i.e., graphite, oxidized Mg, Al, Ni, Fe, Cu, brass), and an X-ray fluorescence tube with multiple targets enabling X-ray line energies such as C Kα (0.277 keV) to Cu Kα (8.04 keV) (Fig. 20). The X-ray tube is typically operated at voltages from a few kV up to 10 kV, with currents ranging up to 650 mA. Filters for optical blocking and X-ray continuum attenuation are insertable just downstream of the gate valve on the source end of the beamline, as are pinholes with 50, 100, and 200 μm diameter hole sizes.

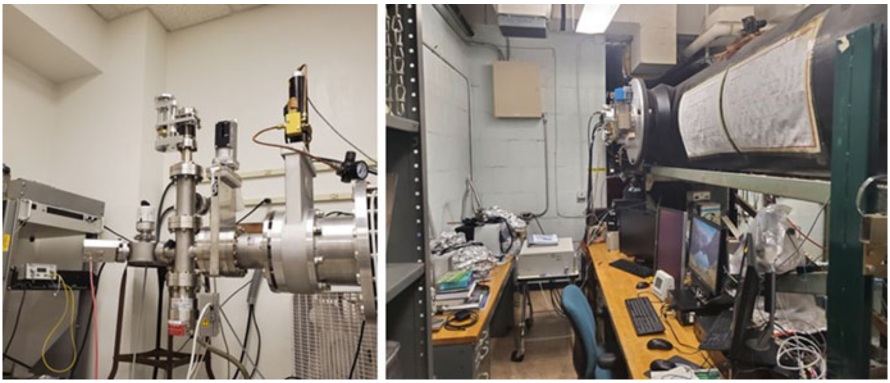

Fig. 20 (Left) Source end of the 47-m long X-ray beamline at PSU. (Right) Control station and a large access port ∼2 m upstream from the instrument insertion end of the beamline. (Credit: PSU)

Asia

The ISAS 30 m X-ray Pencil Beamline (Japan)

The 30-m-long X-ray beam line at the Japanese Institute of Space and Astronautical Science (ISAS) was built with the purpose of evaluating the performance of the X-ray telescope onboard the Astro-D (ASCA) satellite (Kunieda et al., 1993).

Over the past three decades, this facility has been used for ground-based calibrations of the X-ray telescopes on board the ASTRO-E, the ASTRO-E2 (Suzaku), and ASTRO-H (Hitomi) satellites and for performance evaluations of several test optics (Hayashi et al., 2014).

In the ISAS beamline, the Rigaku RA-HF18 HB/LVS X-ray generator (UltraX 18, with the low voltage option) produces a stable X-ray flux with the accelerating voltage of 5–60 kV, from C, Al, Ti, Fe, Cu, Mo, Ag, W, and Pt targets. In order to get a parallel beam, a movable slit is placed 27 m away from the X-ray source. The resultant beam is highly parallel with a rectangular shape.

The beam divergence is 20 arcsec when the slit is 2 mm wide and can be reduced to 8 arcsec with a minimum opening of the slit. To illuminate the entire aperture of the X-ray optics by the fixed X-ray pencil beam, both the telescope and the detectors are moved synchronously.

The telescope and detectors stages are usually called “sample stage” and “detector stage,” respectively. Following the reference system depicted in Fig. 21, the sample stage moves the telescope along Y and Z-axes, rotating around all the 3 axes with automated control. The detector stage can be automatically moved along Y- and Z-axes. Moreover, it can be manually shifted along X-axis in a range of 0.7–9 m from the telescope. The movement range of the sample and detector stages allow telescopes up to 500 mm in size to be fully scanned by the X-ray beam without rotation.

In addition, thin metal filters, a multilayer monochromator, and a double-crystal monochromator are installed in the beam path in order to obtain monochromatic X-rays. The multilayer and double-crystal monochromators are used for 0.9–1.5 keV and 4–18 keV, respectively. Two different detectors are currently available: a conventional gas proportional counter with a 12 mm diameter window, for the

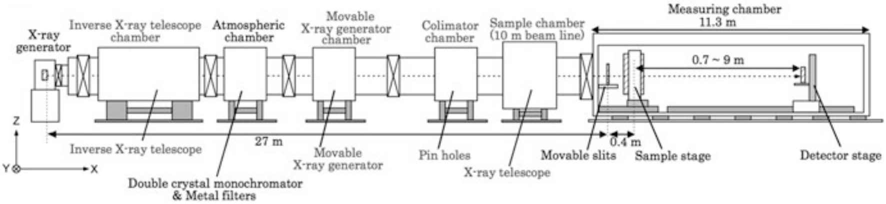

Fig. 21 ISAS beamline. The distance between the X-ray source and the collimating slit is 27 m. (Credit: ISAS)

purposes of the spectral measures, and a 2048 × 2048 pixel C-MOS (pixel size = 11 μm) for imaging analysis.

The IHEP 100 m X-ray Testing Facility (China)

The X-ray testing facility at the Institute of High Energy Physics (IHEP) was originally designed and built for the development and testing of the first X-ray astronomical Chinese mission, the Hard X-ray Modulation Telescope (HXMT) (Zhang et al., 2020) in 2014. It is currently enabling the Einstein Probe and the enhanced X-ray Timing and Polarimetry mission (eXTP) (Chen et al., 2020) telescope calibrations.

The tube is 100 m long with the inner diameter of 0.6 m, departing from a cylindrical 8 m long chamber with a diameter of 3.4 m (Fig. 22) (Zhao et al., 2018). The operation vacuum level is 5 and 2 × 10^{-7} mbar for the instrument chamber and tube, respectively. This is ensured by a system of dry, turbo, and cryopumps which can achieve the work pressure in less than 4 hours, with the time for 100% pure nitrogen venting being than 12 hours.

Within the vacuum chamber, the X-ray optics are placed on the top of a 4-D manipulator with X-Y travel range of 800 mm, a pitch angle travel range of ±20°, and a loading capacity of 200 kg.

There are several detectors and cameras available for imaging, spectral, and timing analysis, including an Andor DX436, a Color X-ray Camera (CXC), and

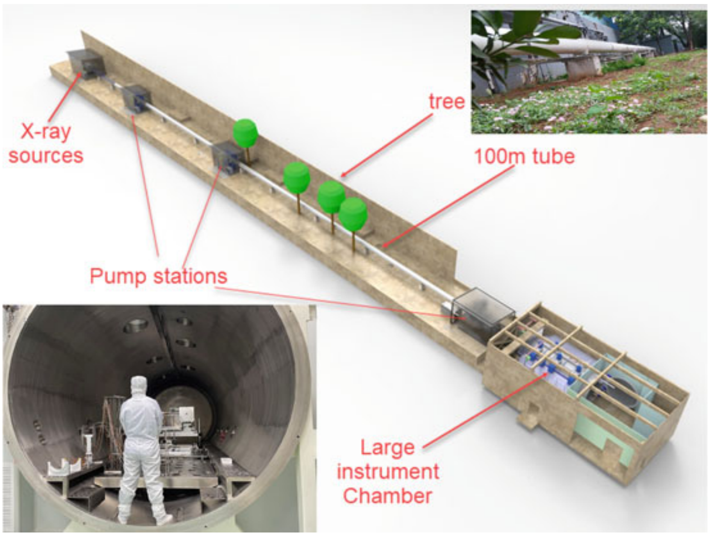

Fig. 22 IHEP facility scheme, with pictures of the outdoor tube and the vacuum chamber. (Credit: IHEP)

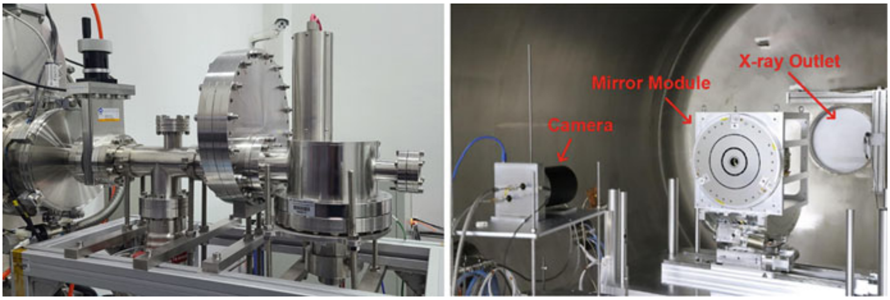

Fig. 23 (Left) The multi-target X-ray source. (Right) The experimental setup within the vacuum chamber, with the big sCMOS X-ray camera in foreground. (Credit: IHEP)

a large sCMOS camera. The DX436 is a 2048 × 2048 CCD camera, sensitive in the soft X-ray. The pixel size is 13.5 µm and readout time 1 fps. The CXC camera is based on a pn-CCD; the ultrafast readout (1000 fps full frame and 3400 fps folded readout) and the very high efficiency on a wide energy range (0.2–30 keV) are its main features. The main characteristics of the sCMOS camera is the size which is 6144 × 6144 pixels, covering an area of 61 × 61 mm^2, big enough to acquire the single reflection of Wolter-I mirror. Beam monitoring and absolute calibration are provided by several Amptek X123 SDDs and CdTe detectors. The detectors are located on two 3D and 6D stages with travel range of 800 mm and a loading capacity of 300 kg. The maximal measurable optics focal length is 5.5 m.

The X-ray beam is produced by a multi-target source (Fig. 23). There are several optional targets and filters for different energies and reduction of continuum, covering the energy range 0.2–20 keV. The facility is also equipped to test and calibrate X-ray focal plane cameras and detectors. For this purpose an X-ray channel cut monochromator covering the 1–40 keV energy band was developed. For the verification of timing performance of detector and telescope system, a modulated X-ray source is also available (Chen et al., 2021). Finally, a polarized X-ray source was developed for the evaluation and calibration of polarized performance of telescope and focal plane detector, like the eXTP PFA.

Synchrotron Radiation Facilities

We have presented, until now, facilities that adopt conventional X-ray sources, positioned at a large distance to reduce the beam divergence. Different X-ray sources are present in synchrotrons accelerators. In these facilities, the X-ray beam is obtained by the travelling of charged particles along a circular path at relativistic speeds: in this case, a very intense, narrow cone of light, parallel to the direction of motion of the charged particles is generated. This artificial light was observed for the first time in 1946 at a General Electric synchrotron accelerator in the USA. Since then, more than 50 synchrotron accelerators around the world were built to produce synchrotron light for experiments, starting with the first that was dedicated to this purpose, built in 1980 in the UK. Table 5 lists some of the major facilities.

Some of the synchrotron facilities have beamlines that are used for calibration or characterization of samples or instruments used in X-ray astronomy. Examples of this type are XPBF 1 (Krumrey et al., 2010) and XPBF 2.0 (Krumrey et al., 2016; Handick et al., 2020) (Fig. 24) of the Physikalisch-Technische Bundesanstalt (PTB) at BESSY II in Berlin, and test facilities at the NSLS, ESRF, and Spring-8.

The X-ray beam produced by these facilities is very narrow. An exception was the synchrotron radiation source (SRS) at the Daresbury laboratory in the UK, which has been closed since 2008, that was used to calibrate the SODART telescopes for the Spectrum Röntgen Gamma satellite. This facility used an asymmetrically cut crystal installed in the beam path (Christensen et al., 1994) to expand the beam to about 200 mm in one direction with a divergence of approximately 20 arcsec. The

Table 5 Synchrotron facilities around the world. (Credits:https://lightsources.org/lightsources-of-the-world/)

Name	Site
Alba	Barcelona, Spain
ALS, Advanced Light Source	Berkeley, California, USA
Argonne National Laboratory	Argonne, Illinois, USA
Australian Synchrotron	Clayton, VIC, Australia
BESSY II, HZB Helmholtz Zentrum Berlin	Berlin, Germany
Canadian Light Source	Saskatoon, Canada
CHESS, Cornell High Energy Synchrotron Source	Ithaca, New York, USA
Diamond	Didcot, UK
Elettra Sincrotrone Trieste	Trieste, Italy
ESRF, European Synchrotron	Grenoble, France
Indus-1, RRCAT	Indore, India
LNLS, Brazilian Synchrotron Light Laboratory	Campinas, SP, Brazil
MAX IV	Lund, Sweden
NSLS-II, Brookhaven National Laboratory	Long Island, New York, USA
NSRRC, National Synchrotron Radiation Research Center	Hsinchu, Taiwan
PAN, Pohang Accelerator Laboratory	Pohang, Korea
PETRA III, DESY	Hamburg, Germany
Photon Factory	Tsukuba, Japan
HZDR, Helmholtz Zentrum Dresden Rossendorf	Grenoble, France
SESAME, Synchrotron-light for Experimental Science and Applications in the Middle East	Allan, Jordan
SOLARIS	Krakow, Poland
SLAC	Menlo Park, California, USA
Spring-8 SACLA	Sayo Town, Japan
Synchrotron Thailand	Nakhon Ratchasima, Thailand
PSI, Paul Sherrer Institute	Villigen, Switzerland

Fig. 24 X-ray parallel beam facility (XPBF 2.0, in operation since 2016) of the Physikalisch-Technische Bundesanstalt (PTB) at BESSY II in Berlin. (Credit: PTB)

idea of using asymmetrically cut crystal is now further developed for the realization of the new facility BEaTriX (section "BEaTriX at INAF-OABrera (Italy)").

Remarks Concerning Existing X-ray Facilities

Three important considerations for calibrating X-ray telescopes are that:

1. The beam divergence should be as small as possible, to simulate an astronomical source.
2. The beam should be large, to cover the full aperture of the optics under test.
3. The experimental chamber size should be commensurate with the articles to be tested: large to accommodate sizeable mirrors and mirror assemblies or small if one wants to minimize the evacuation time.

A comparison of the relevant parameters for several major facilities is provided in Table 6.

Future X-ray telescopes are very large and are fabricated with a modular approach. X-ray measurements need to be performed both on the modules (and single optics) and on the final mirror assembly.

The calibration of the mirror assembly typically requires a facility with a large-diameter vacuum chamber and an X-ray source at a very long distance to measure an accurate telescope effective area. In the case of ATHENA, this means that an X-ray source at a distance of around 800 m is desired. At the moment, such a facility does not exist. A new facility, or a new facility concept, is needed.

On the other hand, the calibration of smaller modules, which comprise the larger mirror assembly, as in the case of the ATHENA telescope, is better accommodated by a facility with a small experimental chamber, which minimizes the evacua-

Table 6 Comparing key parameters of existing X-ray calibration facilities

Facility	Source distance	Beam size	Beam divergence	Instr. chamber size
PANTER	120 m	1 m	859 arcsecs	⊘ = 3.5 m, L = 12 m
XRCF	518 m	1.46 m	291 arcsecs	⊘ = 7.0 m, L = 23 m
MSFC 100-m	104 m	1.3 m	1289 arcsecs	⊘ = 3.0 m, L = 10 m
GSFC 100-m	100 m	0.6 m	619 arcsecs	⊘ = 2.0 m, L = 9 m
XPBF@BESSY II	29 m	up to 7.5×7.5 mm^2	< 2 arcsecs	⊘=0.7 m, L = 1 m
	(collimating mirror)			

tion/venting time. The XPBF 2.0 beam line of the BESSY II synchrotron radiation facility has a well-suited experimental chamber, for example. The X-ray beam is small, and one cannot illuminate the entire pupil in a single shot. However, due to the high photon flux density of around 10^{13} s^{-1} and the existing mechanics, the PSF of the modules can be measured within a short time.

Future Facilities

BEaTriX at INAF-OABrera (Italy)

The testing of the Silicon Pore Optics (SPO) mirror modules (MM) for ATHENA is performed, at the moment, using two facilities:

- The XPBF 2.0 beamline of the BESSY II synchrotron radiation facility (Krumrey et al., 2016), where the experimental chamber is small and allows for short evacuated times. Because of the narrow X-ray beam, the high photon flux density, and the precise mechanics, the PSF of the module is determined by measuring sub-portions of the entrance pupil of the MM and reconstructed via software analysis. Additionally, a direct measurement of the MM effective area cannot be made.
- The PANTER facility (Bradshaw et al., 2019), where the beam fully illuminates the entrance pupil, does not allow a fast evacuation and venting due to the large vacuum chamber size. This is an issue as there are many ($\sim$ 600) mirror modules that require characterization.

Measuring the PSF and effective area of the 600 MMs of the ATHENA telescope (Bavdaz et al., 2021; Collon et al., 2021) requires a facility with a small volume to be evacuated, in order to permit a test rate as fast as the production rate (2 MM/day), and with a parallel, monochromatic, large beam fully covering the entrance pupil.

Fig. 25 The BEaTriX laboratory at the site of INAF-OAB in Merate, Italy. (Credit: INAF-OAB)

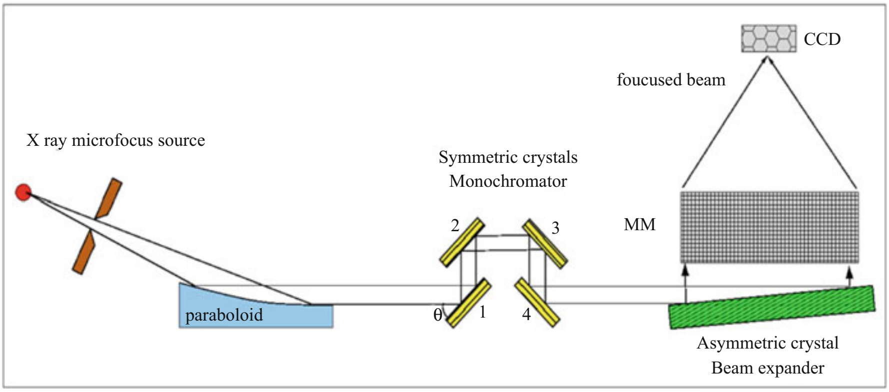

Fig. 26 The BEaTriX optical design. (Credit: INAF-OAB)

For this goal, INAF Osservatorio Astronomico Brera is building a unique facility, BEaTriX (Beam Expander Testing X-ray), at its site in Merate, Italy (Salmaso et al., 2021). By the time this Handbook is written, the first beamline, operating at the energy of 4.51 keV, will have been completed (Fig. 25).

The full system is enclosed in a vacuum tank reaching 10^{-6} mbar, divided into several compartments, separated by gate valves. Each compartment can be evacuated and vented separately in order to minimize the time required for the MM mounting and removal.

The beam properties of BEaTriX are obtained with the optical design shown in Fig. 26 (Spiga et al., 2021). A parallel X-ray beam (4 mm × 60 mm) emerges from a parabolic mirror (Vecchi et al., 2021) in the focus of an X-ray micro-focus source (with size 35 μm, and anode in titanium). The beam is then diffracted four times on silicon crystals, symmetrically cut with respect to the planes [220]. This creates a highly monochromatic beam with bandwidth 0.03 eV. Such a tight monochromation is necessary to minimize the effect of the energy dispersive properties (Sanchez del Rio et al., 1992) of the following beam expander component. Beam expansion is achieved using an asymmetrically cut silicon crystal [220], with asymmetry angle and Bragg angle chosen to obtain an expansion factor of about 50, thus producing a final beam of size 170 mm $\times$ 60 mm. In this way, a parallel and monochromatic beam fully illuminates the MMs under test and is focused onto a CCD (27.6 mm size, 13.5 μm pixel) placed at a distance of 12 m.

The idea of beam expansion with crystals comes from the setup successfully implemented at the Daresbury synchrotron (Christensen et al., 1994). However, in this case, the beam expansion was limited to a single direction, and the obtained divergence was much larger ($\sim$ 20 arcsec) than what was expected for BEaTriX (less than 2 arcsec).

Measurements of the PSF as a function of the MM temperature will also be possible, due to the presence of a thermal box surrounding the MM (Basso and Salmaso, 2019).

The commissioning of the the 4.51 keV facility is expected to be completed by summer 2022. After the demonstration of the concept for the 4.51 keV X-ray energy, a second beamline will be added to BEaTriX to operate at 1.49 keV.

The Vertical X-ray Raster-Scan Facility (Italy)

Neither the PANTER nor the XRCF X-ray test facilities are suited to provide full illumination measurements of a mirror assembly that is as large as the ATHENA assembly, which has an outer diameter of 2.5 m (12 m focal length). To overcome these limitations, a new facility, called the Vertical X-ray raster-scan facility (VERT-X), has been proposed (Pareschi et al., 2019).

Similar to the BEaTriX facility, the VERT-X design uses a highly collimated point source to produce a parallel X-ray beam. Since the beam amplitude will be much smaller than the ATHENA mirror, the source-collimator system must be rastered across the full mirror assembly for complete calibration. This concept results in the design of a calibration facility much smaller in size (as shown in Fig. 27) with respect to the traditional long tube (Moretti et al., 2019).

The compactness of the VERT-X design has several benefits. First, it allows for a vertical facility geometry. This largely simplifies the ATHENA mirror assembly support and mounting system and reduces the PSF degradation due to the lateral (perpendicular to optical axis) gravity to zero. Second, the location of the facility is not as restrictive as would that of a more traditional long beamline facility, permitting co-location with other project facilities. For example, VERT-X has been designed to be near the ATHENA MA integration facility (Valsecchi et al., 2021a). This would make the direct verification of the performance of the assembled optics much easier during the integration phase. Moreover, the small size of the beam allows one to precisely characterize the contribution of single modules to the overall mirror performance.

In its final design, the system is enclosed in a 20 m high cylindrical vacuum chamber, with the focal-plan on the top. The ATHENA mirror assembly will be positioned at the ground level, with the raster-scan mechanism located $\sim$5 m

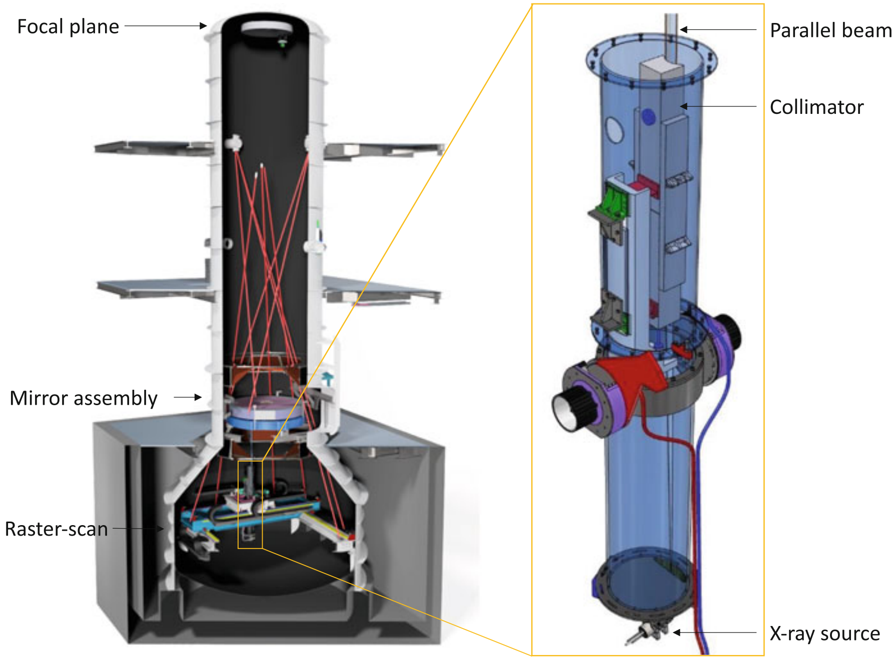

Fig. 27 (Left) Design of the VERT-X facility, with the primary elements labeled. The entire system is within a 20 m-high vacuum chamber, with the X-ray source located at the bottom and the focal plane at the top. Metrology laser beams are shown in red. (Right) The zoomed view on the raster-scan tube which hosts both the collimator and X-ray source. (Credit: ESA, EIE)

underground. In addition to the two translation stages on the horizontal plane, the raster-scan mechanism allows the beam to perform two tilts around the two horizontal axes, in order to point up to 3 degrees off-axis.

The main elements of the VERT-X design are shown in Fig. 27. The raster-scan system consists of four main parts: the base, the X and Y-axis translation frames, and the vertical tube. All these elements are designed in the same material (AISI 304 stainless steel) to have the same thermal behavior as the vessel and to ease the mechanical interface. In particular, the tube hosts the parallelizing collimator and the X-ray source. The optical design of the X-ray collimator is based on a Wolter I configuration of about 1.1 m in length and an average grazing incidence angle of about 0.4 deg. The driving requirements that led to the design are related to the need for sufficiently high reflectivity in the 0.2–12.0 keV energy range and the limitation to 1 arcsec for the divergence error of the collimated beam produced by the mirror.

The mechanical design consists of two separate sections for the parabolic and hyperbolic profiles of the Wolter geometry. The two parts are aligned and held together by means of two plates laterally fixed with adhesive (Fig. 28).

The beam footprint is a portion of a 67 mm radius circular corona 4-mm thick (Fig. 28). Since the beam size, orthogonal to the scan direction, is 60 mm, to cover

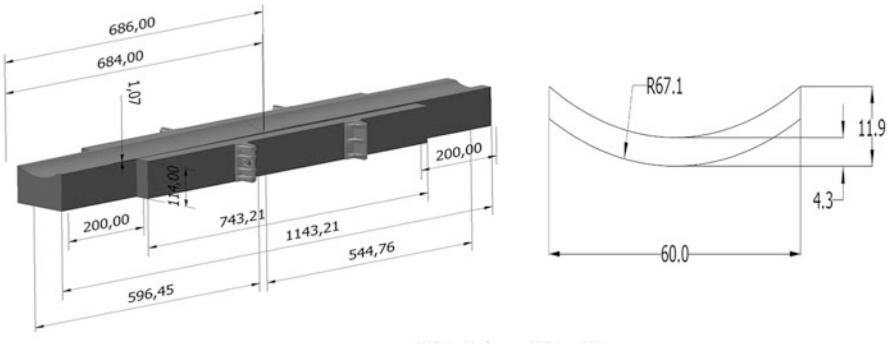

Fig. 28 (Left) The VERT-X collimator is designed to parallelize the beam. (Right) The beam footprint which will cover the ATHENA mirror assembly in 1 hour of raster-scanning. (Credit: ESA, Media Lario)

the ATHENA mirror assembly, a total path length of ∼100 m is needed. With a nominal scan velocity of 30 mm/s, this corresponds to 1 hour, accounting for ∼15 s of settling time at the start and end of each row.

The VERT-X source is required to have a very small size (spot-size ∼ 10 μm), and, at the same time, it must be able to fully operate under vacuum, requiring a liquid-based cooling system. Moreover, the system must not cause vibrations on the raster-scan mechanism, which can only be achieved by an ion-pump for the local vacuum. The anode can be equipped with five different types of materials.

In order to meet the ATHENA calibration needs, the VERT-X beam divergence is required to be <1 arcsec. The primary factors affecting this parameter are the source dimension, the mirror errors, the raster-scan tracking uncertainty, and the relative heat-induced displacement between source and collimator.

While the beam divergence will be the main source of the systematic error in the measurement of the HEW, the statistical uncertain will critically depend on the detector performance. The focal plane will be equipped with a soft X-ray silicon detector with photon counting capabilities, possibly based on back-illuminated sCMOS sensors. In order to accomplish the ATHENA mirror assembly calibration, the required sustainable detector count rate must be at least $>$ 20 photons/s. This would allow for the collection of a sufficient number of photons that would keep the statistical error at the same level as that of the systematic error (Moretti et al., 2019). The detector spectral resolution will allow for the exploitation of the bremsstrahlung continuum for calibration measure purposes.

At the time of writing this Handbook, VERT-X is in the development phase as part of the preliminary definition phase of the ESA ATHENA mission project (Moretti et al., 2021).

Acknowledgments We are very grateful to Marco Barbera (INAF-OAPA, Italy), Wayne Baumgartner (NASA MSFC, USA), Vadim Burwitz (MPE/PANTER, Germany), Abe Falcone (PSU), Takayuki Hayashi (NASA GSFC, USA), Charly Feldman, (UL, UK), Paul O'Brien (UL, UK), Jeff

Kegley (NASA MSFC, USA), Michael Krumrey (PTB Germany), Takashi Okajima (NASA GSFC, USA), Gianpiero Tagliaferri (INAF-OAB, Italy), Alexey Tkachenko (IKI, Russia), Nicholas Thomas (NASA MSFC, USA), and Yusa Wang (IHEP, China) for their valuable support in reviewing this chapter and for giving suggestions.

References

M. Barbera, R. Candia, A. Collura et al., The Palermo XACT facility: a new 35 m long soft X-ray beam-line for development and calibration of next-generation X-ray observatories. Proc. SPIE **6266**, 62663F (2006). https://doi.org/10.1117/12.673004

S. Basso, B. Salmaso, Thermal simulations for characterization of ATHENA Mirror Modules with a radiating box in the BEaTriX facility. Proc. SPIE **11119**, 111191I (2019). https://doi.org/10.1117/12.2530622

S. Basso, D. Spiga, G. Pareschi et al., SIMBOL-X: the problem of the calibrating a 0.5–80 keV 20 m focal length focussing telescope. Proc. SPIE **6688**, 66880J (2007). https://doi.org/10.1117/12.73397

W.H. Baumgartner, B. Ramsey, N. Thomas et al., Ground calibration of the IXPE optics and telescope. Proc. SPIE **11822**, 118210N (2021). https://doi.org/10.1117/12.2595387

M. Bavdaz, E. Wille, M. Ayre et al., ATHENA X-ray optics development and accommodation. Proc. SPIE **11822**, 1182205 (2021). https://doi.org/10.1117/12.2594689

M. Bradshaw, V. Burwitz, G. Hartner et al., Developments in testing X-ray optics at MPE's PANTER facility. Proc. SPIE **11119**, 1111916 (2019). https://doi.org/10.1117/12.2531709

D.N. Burrows, J.A. Nousek, G.D. Berthiaume et al., Search for soft X-ray emission from SN 1987A with a CCD X-ray imaging spectrometer. Astrophys. J. **347**, 1114–1118 (1989)

V. Burwitz, M. Bavdaz, G. Pareschi et al., In focus measurements of IXO type optics using the new PANTER X-ray test facility extension. Proc. SPIE **8861**, 88611J (2013). https://doi.org/10.1117/12.2023309

V. Burwitz, R. Willingale, C. Pelliciari et al., Developing, testing, and calibrating the ATHENA optics at PANTER. Proc. SPIE **10399**, 103990O (2017). https://doi.org/10.1117/12.2274237

Y. Chen, Cui W. W., D.W. Han et al., Status of the follow-up X-ray telescope onboard the Einstein Probe satellite. Proc. SPIE **11444** (2020). https://doi.org/10.1117/12.927280

C. Chen, S. Xiao, S. Xiong et al., Design and test of a portable Gamma-Ray Burst simulator for GECAM. Exp. Astron. **52**(1–2), 45–58 (2021)

F. Christensen, A. Hornstrup, P. Frederiksen et al., Expanded beam X-ray optics calibration facility at the Daresbury Synchrotron. Proc. SPIE **2011**, 540 (1994). https://doi.org/10.1117/12.167225

M. Collon, M. Babic, N. Barriere et al., X-ray mirror development and production for the Athena telescope. Proc. SPIE **11852**, 118521Z (2021). https://doi.org/10.1117/12.2599339

E. Handick, L. Cibik, Krumrey et al., Upgrade of the X-ray parallel beam facility XPBF 2.0 for characterization of silicon pore optics. Proc. SPIE **11444**, 114444G (2020). https://doi.org/doi.org/10.1117/12.2561236

T. Hayashi, T. Sato, K. Tomikawa et al., Upgrade of the thirty-meter X-ray pencil beam line at the Institute of Space and Astronautical Science. Proc. SPIE **9144**, 91444 (2014). https://doi.org/10.1117/12.2055741

R. Iizuka, T. Hayashi,Y. Maeda et al., Ground-based X-ray calibration of the Astro-H/Hitomi soft X-ray telescopes. J. Astronom. Telescopes Instrum. Syst. **4**(1), 011213 (2018). https://doi.org/10.1117/1.JATIS.4.1.011213

J. Kegley, M. Baker, J. Carpenter et al., Improved cryogenic testing capability at Marshall Space Flight Center's X-ray Cryogenic Facility. Proc. SPIE **6265**, 62654E (2006). Space Telescopes and Instrumentation I: Optical, Infrared, and Millimeter. https://doi.org/10.1117/12.672096

M. Krumrey, L. Cibik, P. Müller et al., X-ray pencil beam facility for optics characterization. Proc. SPIE **7732**, 77324O (2010). https://doi.org/10.1117/12.857335

M. Krumrey, P. Müller, L. Cibik et al., New X-ray parallel beam facility XPBF 2.0 for the characterization of the silicon pore optics. Proc. SPIE **9905**, 99055N (2016). https://doi.org/10.1117/12.2231687

H. Kunieda, Y. Tsusaka, H. Suzuki et al., Thirty-meter X-ray pencil beam line at the Institute of Space and Astronautical Science. JJAP **32**, 4805 (1993). https://doi.org/10.1143/JJAP.32.4805

B. Menz, C. Braig, H. Bräuninger et al., Large area X-ray collimator – the zone plate approach. Appl. Opt. **54**(26), 7851–7858 (2015). https://doi.org/10.1364/AO.54.007851

A. Moretti, G. Pareschi, M. Uslenghi et al., VERT-X: VERTical X-ray raster-scan facility for ATHENA calibration. The concept design. Proc. SPIE **11119**, 111190 (2019). https://doi.org/10.1117/12.2530713

A. Moretti, G. Pareschi, Basso, S. et al., The VERT-X calibration facility: development of the most critical parts. Proc. SPIE **11822**, 118220 (2021). https://doi.org/10.1117/12.2593670

S.L. O'Dell, M. Baker, J.M. Carter et al., X-ray testing Constellation-X optics at MSFC's 100-m facility. Proc. SPIE **5168** (2004). https://doi.org/10.1117/12.509584

T. Okajima, Y. Soong, E. Balsamo et al., Performance of NICER flight X-ray concentrator. Proc. SPIE **9905** (2016). https://doi.org/10.1117/12.2234436

G. Pareschi, A. Moretti, B. Salmaso et al., A vertical facility based on raster scan configuration for the X-ray scientific calibrations of the ATHENA optics. Proc. SPIE **11180**, 1118025 (2019). https://doi.org/10.1117/12.2535996

M. Pavlinsky, A. Tkachenko, V. Levin et al., On-ground calibration of the ART-XC/SRG mirror system and detector unit at IKI. Part I. Exp. Astron. **45**(3), 315–350 (2018)

B. Salmaso, S. Basso, V. Cotroneo et al., Building the BEaTriX facility for the ATHENA mirror modules X-ray testing. Proc. SPIE **11822**, 118220M (2021). https://doi.org/10.1117/12.2594182

M. Sanchez del Rio, F. Cerrina, Asymmetrically cut crystals for synchrotron radiation monochromators. Rev. Sci. Instrum. **63**, 936 (1992). https://doi.org/10.1063/1.1143785

H.W. Schnopper, M. Barbera, E. Silver et al., Thin, plastic shell, X-ray optics: an update. Proc. SPIE **4851** (2003). https://doi.org/10.1117/12.461286

D. Spiga, M. Barbera, A. Collura et al., Realization and drive tests of active thin glass X-ray mirrors. Proc. SPIE **9965**, 996509 (2016). https://doi.org/10.1117/12.2231284

D. Spiga, B. Salmaso, S. Basso et al., Performance simulations for the ground-based, expanded-beam X-ray source BEaTriX. Proc. SPIE **11837**, 118370O (2021). https://doi.org/10.1117/12.2595033

Y. Stockman, P. Barzin, H. Hansen et al., XMM flight model mirror module testing. Proc. SPIE **3766** (1999). https://doi.org/10.1117/12.363663

M. Tashiro, H. Maejima, K. Toda et al., Status of X-ray Imaging and Spectroscopy Mission (XRISM). Proc. SPIE 11444 (2020). https://doi.org/10.1117/12.2565812

N.E. Thomas, W. Baumgartner, P.R. Champey et al., The Marshall 100-meter X-ray Beamline. Proc. SPIE **11822**, 118220P (2021). https://doi.org/10.1117/12.2594966

V. Tichy, M. Barbera, A. Collura et al., Tests of lobster eye optics for small space X-ray telescope. NIMA **633**, S169–S171 (2011). https://doi.org/10.1016/j.nima.2010.06.157

J.P. Tock, I. Domken, J.P. Macau, Status of XMM Test Programme in CSL EUV and X-Ray Test Facility (FOCAL X) (1988) https://www.researchgate.net/publication/228601628_Status_of_XMM_Test_Programme_in_CSL_EUV_and_X-Ray_Test_Facility_Focal_X

G. Valsecchi, G. Bianucci, F. Marioni et al., Integration facility for the ATHENA X-ray telescope. Proc. SPIE **11119**, 111190 (2021a). https://doi.org/10.1117/12.2528731

G. Valsecchi, G. Bianucci, F. Marioni, Facility for alignment, assembly, and integration of the SPO mirror modules onto the ATHENA telescope. Proc. SPIE **11822**, 118220J (2021b). https://doi.org/10.1117/12.2593721

G. Vecchi, V. Cotroneo, M. Ghigo et al., Manufacturing and testing of the X-ray collimating mirror for the BEaTriX facility. Proc. SPIE **11822**, 118220N (2021). https://doi.org/10.1117/12.2594581

C.L. Wyman, D.B. Griner, G.H. Hunt et al., Analysis and experimental measurement of straylight suppression systems for the large space telescope. Opt. Eng. **14**(6), 146528 (1975). https://doi.org/10.1117/12.7971787

S. Zhang, F.J. Lu, S.N. Zhang et al., Introduction to the hard X-ray modulation telescope. Proc. SPIE **9144** (2020). https://doi.org/10.1117/12.2054144

Z. Zhao, Y. Wang, L. Zhang et al., Experiments and simulation of Wolter-I focusing mirror. Opt. Precis. Eng. **27**(11), 2330 (2019)